HHS Public Access

Author manuscript

Nat Struct Mol Biol. Author manuscript; available in PMC 2012 April 30.

Published in final edited form as:

Nat Struct Mol Biol. ; 18(11): 1259–1267. doi:10.1038/nsmb.2147.

An asymmetric interface between the regulatory particle and core particle of the proteasome

Geng Tian[1], **Soyeon Park**[1], **Min Jae Lee**[1,2], **Bettina Huck**[1], **Fiona McAllister**[1], **Christopher P. Hill**[3], **Steven P. Gygi**[1], and **Daniel Finley**[1]

[1]Department of Cell Biology, Harvard Medical School, 240 Longwood Ave., Boston, MA 02115, USA

[2]Department of Applied Chemistry, Kyung Hee University, 1 Seocheon-dong, Giheung-gu, Yongin-si, Gyeonggi-do,446-701, Republic of Korea

[3]Department of Biochemistry, University of Utah School of Medicine, Salt Lake City, UT 84112, USA

Abstract

The *S. cerevisiae* proteasome comprises a 19-subunit regulatory particle (RP) and 28-subunit core particle (CP). To be degraded, substrates must cross the CP-RP interface, a site of complex conformational changes and regulatory events. This interface includes two aligned heteromeric rings: the six ATPase (Rpt) subunits of the RP and the seven α subunits of the CP. Rpt C-termini bind intersubunit cavities of the α ring, thus directing CP gating and proteasome assembly. We used crosslinking to map the Rpt C-termini to the α subunit pockets. This reveals an unexpected asymmetry: one side of the ring shows 1:1 contacts of Rpt2–α4, Rpt6–α3, and Rpt3–α2, whereas, on the opposite side, the Rpt1, Rpt4, and Rpt5 tails each crosslink to multiple α pockets. Rpt-CP crosslinks are all sensitive to nucleotide, implying that ATP hydrolysis drives dynamic alterations at the CP-RP interface.

Keywords

proteasome; ubiquitin; AAA protein; crosslinking

INTRODUCTION

The proteasome plays a central role in ubiquitin-dependent protein degradation. Its substrates likely number in the hundreds and, given that they are involved in diverse pathways such as cell cycle control, DNA repair, transcription, and inflammation, the

Correspondence should be addressed to D.F., daniel_finley@hms.harvard.edu.

Author contributions

G.T., S.P., C.P.H., and D.F. contributed to the conception of this project. G.T., S.P., and B.H. contributed to strain construction and genetic analysis. G.T, S.P., and M.J.L. performed crosslinking studies. F.M. and S.P.G performed mass spectrometry on crosslinked samples. G.T., C.P.H. and D.F. were largely responsible for the manuscript.

proteasome functions as an integral component of many cellular regulatory mechanisms. Accordingly, its activity is under intricate control[1–3].

The proteasome core particle (CP, or the 20S proteasome) is a barrel-like complex of four stacked heptameric rings of subunits, with the proteolytic active sites facing the interior space[4]. Substrates gain entry to the CP's interior via a gated axial channel[5–12]. Disruption of the gate enhances ubiquitin-dependent protein degradation in yeast[13]. The channel is formed by the outermost subunits of the CP, which constitute the α rings, while the proteolytic sites are found in the central β rings. The eukaryotic proteasome is thought to have evolved from a simpler complex, which may have resembled the present-day PAN (proteasome-activating nucleotidase) protease complex of archaea[14–17]. The CP of both the PAN protease complex and the eukaryotic proteasome have an $\alpha_7\beta_7\beta_7\alpha_7$ structure, but in the former the rings are homomeric, whereas in the latter they are heteromeric.

The proteasome regulatory particle (RP, also known as the 19S particle and PA700) pairs with the CP to form the proteasome holoenzyme (the 26S complex). The RP can be divided into a CP-proximal ten-subunit base assembly and a distal nine-subunit lid assembly[1,18]. Like the CP, the RP contains subunits that are related to the PAN complex. However, PAN is a homohexameric ATPase ring complex, whereas the RP includes a heterohexameric ATPase ring as a part of the base. In yeast, this "Rpt ring" is formed by Rpt1–Rpt6. Other RP components are poorly understood, but several appear to mediate the recognition and disassembly of ubiquitin chains[1]. ATP hydrolysis by the Rpt ring drives unfolding of protein substrates[2,19–21]. In the majority of PAN complexes only two ATP molecules are bound per ring, with two subunits being bound to ADP and two unoccupied[14]. The Rpt ring is thought to pull substrates into its central pore with sufficient force to promote unfolding of substrate structural domains that are too large to traverse the pore[22,23]. Continued translocation directs the unfolded substrate from the RP channel into the CP, where it is degraded.

Recent studies of the archaeal PAN complex and the related actinobacterial protease ARC have provided major structural insights[15,16]. PAN was found to be a trimer of dimers, at least within its CP-distal oligonucleotide-oligosaccharide binding (OB) and coiled-coil (CC) domains. Accordingly, the eukaryotic Rpt ring assembles via dimeric precursors (Rpt1 and Rpt2, Rpt 4 and Rpt5, and Rpt 3 and Rpt6)[24–26].

The C-terminal segments, or tails, of the Rpt proteins are conserved in evolution (Supplementary Fig. 1a) and critical for proteasome function. They extend from the body of the Rpt ring towards the CP and insert into pockets formed at α–α subunit interfaces[9]. For some tails, insertion results in opening of the CP channel[5–8,27]. The tails also regulate RP assembly in yeast[28,29], and the RP–CP interaction[30,31], most likely via insertion of the tails into the α pockets of the CP[32]. There are six Rpt tails and seven α pockets, a symmetry mismatch indicating that not all α pockets can be simultaneously occupied in this manner. Despite the critical roles played by the RP–CP interface, its organization has remained unknown.

In this study, we use mutagenesis and cysteine-specific crosslinking to probe contacts between the Rpt proteins and the CP α subunits. The results define the relative arrangement

of the 13 subunits that make up the stacked ring assemblies of the RP-CP interface, and reveal that this interface is unexpectedly asymmetric. Three neighboring Rpt proteins insert into specific α pockets, whereas, on the opposite side of the Rpt ring, each Rpt tail can be found crosslinked to more than one α pocket. These results suggest the existence of several interconvertable populations of proteasomes, which differ in the positioning of the unoccupied α pocket. Our findings may explain specific characteristics of the structure of the proteasome as observed by electron microscopy[17,33–35]. Nucleotide affects crosslinking efficiency for every α–Rpt pair, suggesting that the engagement between α and Rpt subunits is dynamically regulated by ATP hydrolytic cycles, with the principal stabilizing contacts alternating from subunit to subunit as ATP is bound and hydrolyzed asynchronously.

RESULTS

The RP-CP Interface

Chemical crosslinking was used to investigate the interaction between the Rpt and α subunits. We first substituted Cys in place of the C-terminal residue of each Rpt protein, which is a critical residue for both the assembly and gating functions of the Rpt tails[8,9,29] (see Supplementary Fig. 1a for sequence alignments of Rpt C-termini). Its key feature is thought to be the main chain carboxylate, rather than the side chain[5,6,8,9]. Each carboxylate is proposed to form a salt bridge to the ε-amino group of a specific α subunit lysine residue[9], a residue that, for six of the seven α subunits, aligns withK66 in the α subunit of the PAN complex (the “pocket lysine”). Accordingly, deletion of the C-terminal residue has substantial phenotypic effects for most Rpts[29]. Substitution mutations, which likely preserve the salt bridge to the pocket lysine, are for the most part well tolerated, though under conditions of proteolytic stress, such as high temperature, hypomorphic function can be observed (Supplementary Fig. 2 and data not shown). Analysis of purified proteasomes from these mutants indicated that the RP–CP interaction is, depending on context, either not detectably perturbed or minimally perturbed (Supplementary Fig. 2).

The introduction of cysteines into the α-ring was guided by the structure of a complex between PA26 and the yeast CP[9]. PA26 is a homoheptameric activator of the CP. Although unrelated to the RP, PA26 also binds the CP via C-terminal tail insertion into the α pockets, and has served as a model for RP–CP interactions[6,9]. In particular, PA26 C-termini form salt bridges with the pocket lysines. Thus, a residue in the α pocket that is proximal to the C-terminus of PA26 was substituted. This residue is directly adjacent to the beginning of the α2 helix in each α subunit, and is surface-exposed on the interior of the pocket(Fig. 1; for an alignment of α subunits in this region, see Supplementary Fig. 1b). Cysteines were individually introduced into each α subunit. These α subunit mutants were then crossed to the *rpt* mutants to create a 6×7 array of double Cys substitution mutants. All double mutant combinations were viable (Supplementary Fig. 2 and data not shown).

Identification of two α–Rpt subunit pairs

Crosslinking was carried out using the divalent cysteine crosslinker Bis-maleimidoethane (BMOE), whose spacer arm is 8-Å when extended[36,37]. To ensure that BMOE will only generate crosslinks to Rpt tails that insert into a given α pocket, we modeled the space that

could be searched by a BMOE molecule anchored at the introduced Cys residue, using the crystal structure of the yeast CP. The results indicated that the Rpt tails must gain access to the pocket to achieve crosslink formation.

An initial scan for crosslinked products in whole-cell lysates allowed mapping of α–Rpt subunit pairings α1-Rpt4 and α5-Rpt1 (Fig. 2a and 2b). For example, a crosslink product was found to form in Rpt4-L437C α1-I87C double mutant proteasomes, but not in double mutants between α1-I87C and Cys substitutions of other Rpt proteins (Fig. 2a). The crosslink product was visualized via 6xHA epitopes appended to the α subunits at their C-termini, which are surface-exposed (Supplementary Fig. 3). The apparent molecular mass of the crosslinked products, approximately 80kD, is consistent with an adduct between Rpt4 (49kDa) and α1 (28kDa) (Fig. 2a).

To understand the crosslinking data, it is important to recognize that each α pocket is formed at the interface of two α subunits. Within any αX–αY pocket, the penultimate residue of the Rpt is expected to displace the Pro17 turn of αX, which promotes repositioning of the α subunit N-termini to form an open gate conformation[5–7], while the Rpt C-terminal carboxylate is expected to form a salt bridge with the pocket lysine residue of subunit Y[5,6,9] (Fig. 1). The cysteine substitution is placed in subunit αY(α5 in Fig. 1), with which the C-terminal three residues of PA26, and presumably Rpt subunits, form main chain hydrogen bonding interactions. Thus, in the case of Rpt1for example, crosslinking to α5 indicates that Rpt1 might affect the state of the Pro17 turn and N-termini of α4. Consequently, we use the names of both subunits when referring to an α pocket. The pockets are α1–α2, α2–α3, α3–α4, α4–α5, α5–α6, α6–α7, and α7–α1.

The finding that the Rpt4 C-terminus inserts into the α7–α1 pocket was unexpected, given the sequence characteristics of this pocket. Because there are six Rpt proteins apposed to seven α subunits, one of the α pockets must be unoccupied at a given time, or at least not occupied by an Rpt C-terminus. The α7–α1 pocket was previously hypothesized to be the "empty" pocket of the α ring because it lacks a pocket lysine[9] (Supplementary Fig. 1b).

To test whether the α1–Rpt4 and α5–Rpt1 crosslinks were generated in mature, fully-assembled proteasomes, we repeated the crosslinking with affinity-purified proteasomes. Proteasomes were purified from wild-type cells, α1-I87C mutants, Rpt4-L437C mutants, and the corresponding double mutants. The pattern of crosslinking was similar to that seen in whole cell extracts, and in addition we observed that crosslinking was strictly dependent on the presence of both α1-I87C and Rpt4-L437C substitutions (Fig. 2c). When these reactions were probed with antibodies to Rpt4, the specificity of the crosslink for the mutated form of α1 was also apparent (Fig. 2e). Similar experiments confirmed insertion of Rpt1 into the α4–α5pocket (Fig. 2d and 2f).

Identification of an α4–Rpt2 pair

A third crosslink observed in whole-cell lysates was between α4 and Rpt2 (Fig. 3a). We purified proteasomes from the α4–Rpt2 double mutant and the corresponding single mutants, and repeated the crosslinking. Although crosslink formation was fully dependent on Rpt2-L437C, it proved to be only partially dependent on the α4-N79C substitution (Fig.

3b and 3c). This result suggested that a native Cys residue in α4 might be capable of crosslinking to Rpt2. We therefore examined the structure of the α3–α4 pocket, modeling its interaction with Rpt tail elements on the PA26–yeast CP co-crystal structure. As suspected, two native cysteines (Cys32 and Cys46) in α4 were potentially accessible to the C-terminal tail in its modeled position, with Cys46 being the more surface-exposed of the two (Fig. 3d). If some structural flexibility of the Rpt2 tail within the pocket is assumed, Cys46 should not be too distant from the tail to be crosslinked.

To test whether Cys32 or Cys46 might account for the unidentified crosslinks, we tested HA-tagged but otherwise wild-type α4 for crosslinking to the standard panel of Rpt Cys mutants. In whole-cell extracts we again observed specific crosslinking to Rpt2, supporting the involvement of native Cys residues in crosslink formation (Fig. 3e). Cys32 and Cys46 were therefore jointly substituted with alanine. Under these conditions, α4–Rpt2 crosslinking was fully dependent on the α4-N79C substitution (Fig. 3f and g). Thus, cysteine residues at multiple positions within the α3–α4 pocket can apparently crosslink to Rpt2.

α3–Rpt6 and α2–Rpt3 pairs

The data above, together with the known subunit arrangement of the Rpt ring[38] (Supplementary Fig. 4), constrain the possible assignments of the remaining three α–Rpt pairs. For example, because α3 abuts α4 and Rpt6 abuts Rpt2, the α4–Rpt2 pair should be flanked by an α3–Rpt6 pair; that is, the Rpt6 tail is expected to insert into the α2–α3 pocket. However, when crosslinking was carried out in whole-cell extracts from early stationary phase cells, we reproducibly observed contacts between α3 and Rpt2 and Rpt3, in addition to Rpt6 (Fig. 4a). In contrast, whole-cell extracts from exponential phase cells yielded only the expected α3–Rpt6 crosslink (Fig. 4b). Purified proteasomes from stationary phase cells exhibited crosslinking only between α3 and Rpt6, and these crosslinks required both α3-T81C and Rpt6-K405C substitutions (Fig. 4c–e). In summary, our data indicate that the α2–α3 pocket is the receptor for the Rpt6 tail, and also provide an initial indication that under some physiological conditions Rpt–α pocket mispairing or ambiguity might occur. The mispaired Rpt C-termini, Rpt2 and Rpt3, flank Rpt6 on either side. An interesting possibility is that ambiguous alignment of the Rpt6 tail is characteristic of certain proteasome assembly intermediates.

Assignment of the α3–Rpt6 pair implies that an α2–Rpt3 pair should be formed in the next position, working clockwise around the ring. In crosslinking studies with crude extracts, we could not visualize this putative species (Supplementary Fig. 5a). However, in purified proteasomes, the predicted crosslinked species could be observed at the correct size (arrow), the formation of which requires the α2-A79C substitution (Fig. 4f). These data support assignment of Rpt3 as a ligand of the α1–α2 pocket. However, the Rpt3-K428C substitution leads to some crosslinking in the absence of α2-A79C, resulting in unidentified background bands that may reduce the intensity of the signal for the α2–Rpt3 pair (Fig. 4g).

The α5–α6 and α6–α7 pockets

The two remaining unassigned α pockets, α5–α6 and α6–α7, showed background crosslink formation to endogenous cysteines (Supplementary Figs. 5b, 5c). The responsible Cys residues were identified and mutated to Ala (Fig. 5a,g). In this genetic background we observed specific crosslinking of the α6–α7 pocket to both Rpt4 and Rpt5, in extracts and with purified proteasomes(Fig. 5b–f). The α5–α6 pocket did not form detectable crosslinks in extracts but crosslinked specifically to Rpt1 and Rpt5in purified proteasomes (Fig. 5h–l).

The results above indicate that several Rpt proteins can crosslink to multiple α pockets. Rpt5, for example, is capable of crosslinking to both α5–α6 and α6–α7 pockets (Fig. 5). Moreover, Rpt4 crosslinks to not only α6–α7 (Fig. 5b–d), but also, as described above, α7–α1 (Fig. 2). Finally, Rpt1 crosslinks to both α5–α6 (Fig. 5i,j) and, as shown in Fig. 2, α4–α5. Thus, the register of tail–pocket insertion is apparently not strictly fixed over four neighboring α pockets, in striking contrast to the remaining three pockets (α1–α2, α2–α3, and α3–α4). Additionally, we found no evidence for a defined unoccupied α pocket, the existence of which has generally been assumed, based on the excess number of α pockets over Rpt tails. Our working model of the RP–CP interface is shown in Fig. 6a–c.

The RP–CP interface is dynamic

ATP hydrolysis by the proteasome is essential for its ability to degrade proteins, and provides the driving force for translocation of the substrate protein through the RP-CP interface. Based on studies of related ATP-dependent proteases, nucleotide hydrolysis presumably drives substrate translocation, at least in part, by guiding movement of the pore-1 loop within the axial substrate translocation channel[21,39,40]. However, far from the pore-1 loop, ATP hydrolysis may also be expected to direct movement of the C-domains, from which the Rpt tails emerge[40,41]. We therefore tested whether the engagement of Rpt tails within their cognate α pockets is regulated by ATP.

Proteasomes were purified in the presence of 0.1 mM ATP and subjected to crosslinking after the addition of ADP, ATP, or ATPγS to 1 mM. We found that all of the α-Rpt contacts behaved similarly in that crosslinking was enhanced by ATP in comparison to ADP (Fig. 7). A trivial explanation for the suppression of crosslinking by ADP would be that ADP drives dissociation of the CP and RP. Previous work has shown that for yeast proteasomes this is not the case[42], and we confirmed under our conditions that little or no dissociation of CP and RP occurs. (Supplementary Fig. 6).

ATPγS, a nonhydrolyzable ATP analog, stimulated α-Rpt crosslinking, in comparison to ATP, for some crosslinking pairs but not others (Fig. 7). These effects were modest in comparison to those seen when comparing ATP to ADP. The α2–α3α3–α4, and α4–α5 pockets, all showing enhanced crosslink formation with ATPγS, form a continuous block of subunits on one side of the Rpt ring – interestingly, the side characterized by fixed Rpt–α crosslinks. Pockets on the opposite face of the ring showed either no stimulation or a slight suppression in the presence of ATPγS. Consistent with these trends, Rpt1 crosslinking to α4–α5 was stimulated by ATPγS but crosslinking to α5–α6 was not. These data suggest that

α–Rpt crosslink formation may serve as a sensitive probe to differentiate subtly different functional states of the mature proteasome holoenzyme.

DISCUSSION

The dynamic nature of the RP–CP interface was first apparent when the substrate translocation channel of the CP was identified and found to assume open and closed states in a regulated manner[11,12]. The organization of this extensive interface has remained unknown, despite fragmentary data from many studies based on either the two-hybrid method, crosslinking, or other approaches[27,30,33,43–48]. In general, these studies can be only partially reconciled with each other and with our current understanding of the topologies of the Rpt and α rings. In contrast to all previous work, we have used mutagenesis to focus exclusively on the contacts between Rpt tails and the α pockets in intact proteasomes. Thus, we have mapped those contacts that are thought to provide the key connections between the RP and the CP. The final map is complete, self-consistent, and compatible with constraints that derive from the known subunit orders of the two rings.

The RP–CP contact points exhibit several unanticipated features. Most importantly, there is a general asymmetry in the mapping, such that on one side of the Rpt ring we observe fixed contacts, whereas on the other side of the ring the C-terminus of an Rpt exhibits flexible contacts, with the capacity to insert into more than one α pocket. The possibility that the flexibility of crosslink formation is in general a peculiarity of BMOE-induced crosslinking was excluded through using other crosslinking methods, including $CuCl_2$-mediated crosslinking[32], in which no linker arm is present (data not shown). As a consequence of the flexibility of Rpt insertion, we did not identify any unoccupied α pocket, although the existence of such a pocket was anticipated based on the Rpt–α subunit symmetry mismatch. Our data suggest a model in which a proteasome sample is composed of distinct sub-populations, each with a different unoccupied pocket. Such subpopulations are likely to interconvert. Thus, an unoccupied pocket, though not fixed or identifiable by crosslinking, may underlie the flexibility in register of Rpt1, Rpt5, and Rpt4. Moreover, the symmetry mismatch between the Rpt and α rings also dictates that the Rpt tail and the α pockets cannot be aligned in such a way that each tail is proximal to a unique pocket (Fig. 6b), since the interpocket angle in the α ring is 51° and the tail-tail angle is on average 60°. This problem could be minimized if only two tails are engaged at a given time[14] (i.e., those tails associated with ATP-bound subunit), but with the engagement of four tails, some tails would be required to straddle two α pockets.

Interestingly, the asymmetrical character of the RP–CP interface is consistent with existing genetic data in that strong phenotypes tend to cluster towards the fixed half of the ring. Among Rpt tail mutants, the strongest phenotype is that of Rpt6, which is fixed to the α2–α3 pocket, whereas the weakest phenotype belongs to Rpt1, which shows flexibility in its pocket insertion(ref. 29 and S.P., unpublished data). Likewise, among the α subunits the α3 mutants show a far more pronounced phenotype than α7 (ref. 12,13). All of the fixed tails – Rpt2, Rpt6, and Rpt3 show strong phenotypes, whether in proteasome assembly or gating[8,29].

The asymmetric character of the RP–CP interface described here may help to explain the misalignment in the axes of the Rpt and α rings observed in electron microscopic analyses of the proteasome. Fig. 6d provides one example[17,33–35]. Most likely the RP axis fluctuates substantially with respect to the CP[49], the misaligned orientation described by Bohn et al[33] being an average of many species. Based on our mapping, the asymmetry arising from this misalignment is well correlated with that of crosslinking; it was concluded that the center of the Rpt ring is displaced in the direction of the α2–α3 pocket[33], which is in the center of the region characterized by fixed crosslinks. Indeed, it is possible that the asymmetry of the CP-RP interface described in this study may also underlie the tilted and misaligned RP-CP orientation in the PAN holoenzyme[17], despite the homomeric nature of PAN and its corresponding α ring.

Although our findings define important parameters, especially regarding the fixed contact points, further aspects of RP–CP interaction require more study. Do Rpt tails that insert into two α pockets have a preferred pocket? Does the choice of pocket influence the functional consequences of tail engagement, such as in the assembly, gating and stability of the proteasome? Does the shift of a tail from one pocket to another occur primarily as a consequence of ATP hydrolysis? Is it true that any one of four distinct pockets can be unoccupied in a given proteasome (α4–α5, α5–α6, α6–α7, and α7–α1) or, for example, if α6–α7 is not occupied by Rpt4 is it always occupied by Rpt5?

The crosslinking approach requires the use of α pocket and Rpt tail mutants, which could affect the specificity of insertion. However, the only phenotypes we found were mild. Another caveat to the crosslinking approach is that it monitors the entry of Rpt tails into the α pocket, but not every instance of tail entry is necessarily a functional engagement. An important goal for future work is to determine the functional significance of asymmetry at the interface and whether this a property of the Rpt tails or some other element of the interface. It will be interesting to find mutants in which the symmetry of the interface is altered.

Proposed role of Rpt–CP contacts in Rpt ring assembly

Mapping of the Rpt–CP contacts also provides new information on assembly of the Rpt ring. Previous studies have suggested that Rpt ring assembly in yeast is guided, in part, by pre-existing α rings[28,29,32]. Of particular importance to this model is that both α subunit mutants and Rpt mutants show the accumulation of Rpt ring assembly intermediates. The Rpt mutants were single amino acid deletions at the C-termini of Rpt4 and Rpt6, the latter displaying a stronger phenotype. To date, only one CP subunit, α3, has been implicated in Rpt ring assembly[32]. This subunit might thus be predicted to directly contact one of the Rpt's that promote assembly, and indeed the tail of Rpt6 crosslinks specifically to α3. This observation provides further support for the idea that the CP promotes Rpt ring assembly in yeast and provides a foundation for more precise studies of this complex assembly pathway.

The asymmetry of the RP–CP interface may also underlie distinct functional differences among the RP chaperones, which bind near the C-termini of four of the Rpt proteins to assist in assembly of the Rpt ring. Rpn14 and Nas6 have been grouped functionally by genetic criteria, and are found on the fixed side of the Rpt ring. Rpn14 and Nas6 can be

distinguished genetically from Hsm3 and Nas2, which lie on the flexible side of the ring[24,26,38]. For Rpn14 and Nas6, prior studies suggest that the chaperone–Rpt interaction is competitive with RP–CP binding[28,29]. The suggested mechanism involves steric hindrance: insertion of the C-terminal tails of the Rpt proteins may be disfavored by the presence of the chaperones, due to the proximity of the chaperones to the CP when they are bound to Rpt proteins[28,29]. A still unidentified release mechanism may obtain for Hsm3 and Nas2 (ref. 25,38,50 and S.P., unpub. data). Thus, insertion of Rpt tails into α pockets of the CP on the flexible side of the ring may be poorly suited to displace the chaperones.

RptC-termini and α subunit N-termini may coevolve

Our data raise the possibility that the C-terminal tails of the Rpt subunits have co-evolved with the N-terminal tails of the α subunits, though they are not in contact with one another. For example, Rpt2 has strong gate-opening ability whereas Rpt4 has not been seen to promote gate opening[8,10,29]. This may be attributed to the HbYX motif of Rpt2 and the absence of one in Rpt4 (ref. 8). But this distinction between Rpt2 and Rpt4 may also result from the nature of the N-terminal tails of the α subunits whose movements they direct. Our crosslinking data indicate that the C-terminal tail of Rpt2, in docking at the α3–α4 pocket, would displace the α3 N-terminal tail from its central position in the closed form of the CP gate (Fig. 8). On the other hand, engagement of the Rpt4 C-terminal tail would potentially lead to displacement of the N-terminal tail of α7. However, deletion of the α7 tail does not open the CP gate, whereas that of α3 does[12]. This difference is consistent with the positioning of these tails within the gate, with α3's tail being the most centrally located of any α subunit and α7's tail being peripheral (Fig. 8). Rpt4 might also influence the α1 N-terminus, which is similarly peripheral (Fig. 8). More generally, it is striking that the N-termini of the α subunits that show flexible crosslinking all point outwards from the CP in the closed state of the complex, whereas those showing fixed crosslink formation all follow an inward or lateral path (see Fig. 8b).

Coupling of gating to nucleotide hydrolysis

The proteasome undergoes cycles of ATP hydrolysis in both the presence and absence of substrate. Thus, the sensitivity of Rpt-α pocket crosslinking to nucleotide suggests that the tail–pocket interaction is dynamic, a conclusion that appears to apply to each Rpt protein. The low crosslinking efficiencies seen in the presence of ADP do not necessarily indicate complete dissociation of the Rpt tail from α pockets or a complete lack of involvement of ADP-bound Rpt proteins in gating. Indeed, ADP is effective in stabilizing RP-CP association, at least for yeast proteasomes[42,51], although whether this effect is related to the engagement of Rpt tails with the CP is not known. The nucleotide-free form of the ATPase might show the most radical changes in orientation of the C-domain, but we cannot as yet probe that state, because wild-type proteasomes dissociate under such conditions.

In accordance with our finding that Rpt tails engage less strongly with the CP in the presence of ADP rather than ATP or ATPγS, we postulate that, as ATP is hydrolyzed by successive subunits in the Rpt ring, the contacts between the RP and CP undergo a cycle of motions in response. Structural studies of related hexameric ATPases suggest that nucleotide is hydrolyzed in a rotary mechanism[52,53], in which one of the highly populated species

contains two ATP molecules and two ADP molecules, with two ATPase subunits not interacting with nucleotide. We favor an analogous model for the proteasome[14]. Our finding that ATP and ADP have distinct effects on the strength of interaction between the Rpt C-termini and the α pockets therefore suggests that strong engagement of only a subset of tails, possibility as few as two, is needed for opening of the CP gate. The Rpt tails that strongly activate the gate – Rpt2, Rpt3, and Rpt5 – alternate around the ring. Consequently, the gate would remain open through cycles of ATP hydrolysis that proceed around the ring, even if ADP and unbound Rpt subunits adopt conformations that do not promote engagement of their C-termini.

METHODS

Yeast strains and media

Procedures for the genetic manipulation of yeast, including transformation and tetrad analysis, were as described[55]. Yeast strains are listed in Supplementary Tables 1 and 2. All strains used in this study are congenic with strain DF5 (*MAT**a**/MATα lys2-801/lys2-801 leu2-3, 2-112/leu2-3, 2-112 ura3-52/ura3-52 his3-Δ200/his3-Δ200 trp1-1/trp1-1*)[56]. Transformation cassettes[57] were used for protein tagging. Standard synthetic defined media, consisting of 0.7% (w/v) Difco Yeast Nitrogen Base supplemented with amino acids, adenine, uracil, and 2% (w/v) dextrose, were used for growth of cells at 30°C unless specified otherwise. Spotting assays were performed as described[58].

Antibodies

The anti-HA antibody was from AbCam (12CA5). Anti-Rpt4 and anti-α4 were from W. Tansey. Anti-Rpt1 and anti-Rpt6 were from C. Mann. Anti-Rpt2, Rpt3, and Rpt5 were from Biomol (PW8260, PW8250, and PW8245, respectively).

Preparation of total cell lysates and crosslinking in total cell lysates

Yeast cells were collected from 5-ml overnight cultures in YPD media and resuspended in 0.5 ml PBS buffer (137 mM NaCl, 2.7 mM KCl, 10 mM Na_2HPO_4, 1.76 mM KH_2PO_4 [pH 7.4]) supplemented with 5mM $MgCl_2$ and 1 mM ATP. 75 μl of glass beads (0.5 mm soda lime, BioSpec, Bartlesville, OK) were added to the solution, and the cells were disrupted by sonication (cycles of 15 s of sonication followed by 15 s on ice over 3 min; S-450 digital sonifier, Branson, Danbury, CT). In one experiment (Fig. 4b), lysis was performed in liquid nitrogen as described[29]. The samples were then centrifuged (1.6×10^4 x *g* for 5 min at 4°C) and the supernatant collected and clarified. The protein concentration was estimated with the Coomassie Plus (Bradford) Protein Assay kit (Thermo Scientific, Rockford, IL) following the manufacturer's instructions, and adjusted to 1 mg ml^{-1}. Crosslinking was achieved by adding 0.1mM BMOE (Bis-Maleimidoethane: Thermo Scientific, Rockford, IL), followed by incubation on ice for one hour[36]. Crosslinking was quenched by addition of 1 mM DTT. The strains used for screening whole-cell lysates by crosslinking are listed in Supplementary Table 2.

Purification and chemical crosslinking of proteasomes

All strains used for proteasome purification have a TEV-protein A tag appended to the C-terminus of Rpn11 (ref. 51). Proteasome purifications were carried out using IgG-Sepharose (MP Biochemical, Solon, OH), with TEV protease (Invitrogen, Carlsbad, CA) used for elution (25mM Tris-HCl [pH7.5], 5mM $MgCl_2$, 1mM ATP; details as described[59] except that $MgCl_2$ was used in all buffers that contained ATP). The crosslinking procedure for purified proteasomes was similar to that for total cell lysates except that the protein concentration was 0.1 mg ml^{-1}. For crosslinking, purified proteasomes (in concentrated stocks in TEV elution buffer) were diluted into PBS supplemented with 5mM $MgCl_2$ and 1mM ATP.

Native PAGE of total cell lysate

Total cell lysates were prepared as described above, and 30 μg of total protein were resolved by 3.5% (w/v) native PAGE, followed by LLVY-AMC overlay assay[60].

Nucleotide-dependence of crosslinking

Proteasomes were purified as described above except that the IgG column elution buffer contained 0.1 mM ATP instead of 1 mM ATP. Proteasomes were pre-incubated with 1 mM ADP, 1 mM ATP or 1 mM ATPγS at room temperature for 30 min before proceeding with same crosslinking protocol as given above.

Supplementary Material

Refer to Web version on PubMed Central for supplementary material.

Acknowledgments

We thank W. Tansey (Vanderbilt University Medical Center, Nashville, TN 37232, USA) and C. Mann (CEA/*Saclay*, F-91191 Gif-sur-Yvette Cedex, France) for antibodies, A. Matouschek for comments on the manuscript, and W. Baumeister for permission to reproduce Fig. 6D. Funding was provided by NIH grants to D.F. (R37GM43601), C.P.H. (R01 GM59135), and S.G. (GM67945). S.P. was supported by a fellowship from the Charles A. King Trust and M.J.L. by the American Health Assistance Foundation.

References

1. Finley D. Recognition and processing of ubiquitin-protein conjugates by the proteasome. Annual review of biochemistry. 2009; 78:477–513.
2. Schrader EK, Harstad KG, Matouschek A. Targeting proteins for degradation. Nature chemical biology. 2009; 5:815–22. [PubMed: 19841631]
3. Demartino GN, Gillette TG. Proteasomes: machines for all reasons. Cell. 2007; 129:659–62. [PubMed: 17512401]
4. Groll M, et al. Structure of 20S proteasome from yeast at 2.4 A resolution. Nature. 1997; 386:463–71. [PubMed: 9087403]
5. Yu Y, et al. Interactions of PAN's C-termini with archaeal 20S proteasome and implications for the eukaryotic proteasome-ATPase interactions. The EMBO journal. 2010; 29:692–702. [PubMed: 20019667]
6. Stadtmueller BM, et al. Structural models for interactions between the 20S proteasome and its PAN/19S activators. The Journal of biological chemistry. 2010; 285:13–7. [PubMed: 19889631]

7. Rabl J, et al. Mechanism of gate opening in the 20S proteasome by the proteasomal ATPases. Molecular cell. 2008; 30:360–8. [PubMed: 18471981]
8. Smith DM, et al. Docking of the proteasomal ATPases' carboxyl termini in the 20S proteasome's alpha ring opens the gate for substrate entry. Molecular cell. 2007; 27:731–44. [PubMed: 17803938]
9. Forster A, Masters EI, Whitby FG, Robinson H, Hill CP. The 1.9 A structure of a proteasome-11S activator complex and implications for proteasome-PAN/PA700 interactions. Molecular cell. 2005; 18:589–99. [PubMed: 15916965]
10. Kohler A, et al. The axial channel of the proteasome core particle is gated by the Rpt2 ATPase and controls both substrate entry and product release. Molecular cell. 2001; 7:1143–52. [PubMed: 11430818]
11. Whitby FG, et al. Structural basis for the activation of 20S proteasomes by 11S regulators. Nature. 2000; 408:115–20. [PubMed: 11081519]
12. Groll M, et al. A gated channel into the proteasome core particle. Nature structural biology. 2000; 7:1062–7. [PubMed: 11062564]
13. Bajorek M, Finley D, Glickman MH. Proteasome disassembly and downregulation is correlated with viability during stationary phase. Current biology : CB. 2003; 13:1140–4. [PubMed: 12842014]
14. Smith DM, Fraga H, Reis C, Kafri G, Goldberg AL. ATP binds to proteasomal ATPases in pairs with distinct functional effects, implying an ordered reaction cycle. Cell. 2011; 144:526–38. [PubMed: 21335235]
15. Zhang F, et al. Structural insights into the regulatory particle of the proteasome from Methanocaldococcus jannaschii. Molecular cell. 2009; 34:473–84. [PubMed: 19481527]
16. Djuranovic S, et al. Structure and activity of the N-terminal substrate recognition domains in proteasomal ATPases. Molecular cell. 2009; 34:580–90. [PubMed: 19481487]
17. Smith DM, et al. ATP binding to PAN or the 26S ATPases causes association with the 20S proteasome, gate opening, and translocation of unfolded proteins. Molecular cell. 2005; 20:687–98. [PubMed: 16337593]
18. Glickman MH, et al. A subcomplex of the proteasome regulatory particle required for ubiquitin-conjugate degradation and related to the COP9-signalosome and eIF3. Cell. 1998; 94:615–23. [PubMed: 9741626]
19. Weber-Ban EU, Reid BG, Miranker AD, Horwich AL. Global unfolding of a substrate protein by the Hsp100 chaperone ClpA. Nature. 1999; 401:90–3. [PubMed: 10485712]
20. Sauer RT, Baker TA. AAA+ Proteases: ATP-Fueled Machines of Protein Destruction. Annual review of biochemistry. 2011; 80:587–612.
21. Glynn SE, Martin A, Nager AR, Baker TA, Sauer RT. Structures of asymmetric ClpX hexamers reveal nucleotide-dependent motions in a AAA+ protein-unfolding machine. Cell. 2009; 139:744–56. [PubMed: 19914167]
22. Aubin-Tam ME, Olivares AO, Sauer RT, Baker TA, Lang MJ. Single-molecule protein unfolding and translocation by an ATP-fueled proteolytic machine. Cell. 2011; 145:257–67. [PubMed: 21496645]
23. Maillard RA, et al. ClpX(P) generates mechanical force to unfold and translocate its protein substrates. Cell. 2011; 145:459–69. [PubMed: 21529717]
24. Saeki Y, Toh EA, Kudo T, Kawamura H, Tanaka K. Multiple proteasome-interacting proteins assist the assembly of the yeast 19S regulatory particle. Cell. 2009; 137:900–13. [PubMed: 19446323]
25. Kaneko T, et al. Assembly pathway of the Mammalian proteasome base subcomplex is mediated by multiple specific chaperones. Cell. 2009; 137:914–25. [PubMed: 19490896]
26. Funakoshi M, Tomko RJ Jr, Kobayashi H, Hochstrasser M. Multiple assembly chaperones govern biogenesis of the proteasome regulatory particle base. Cell. 2009; 137:887–99. [PubMed: 19446322]
27. Gillette TG, Kumar B, Thompson D, Slaughter CA, DeMartino GN. Differential roles of the COOH termini of AAA subunits of PA700 (19 S regulator) in asymmetric assembly and activation of the 26 S proteasome. The Journal of biological chemistry. 2008; 283:31813–22. [PubMed: 18796432]

28. Roelofs J, et al. Chaperone-mediated pathway of proteasome regulatory particle assembly. Nature. 2009; 459:861–5. [PubMed: 19412159]
29. Park S, et al. Hexameric assembly of the proteasomal ATPases is templated through their C termini. Nature. 2009; 459:866–70. [PubMed: 19412160]
30. Kumar B, Kim YC, DeMartino GN. The C terminus of Rpt3, an ATPase subunit of PA700 (19 S) regulatory complex, is essential for 26 S proteasome assembly but not for activation. The Journal of biological chemistry. 2010; 285:39523–35. [PubMed: 20937828]
31. Thompson D, Hakala K, DeMartino GN. Subcomplexes of PA700, the 19 S regulator of the 26 S proteasome, reveal relative roles of AAA subunits in 26 S proteasome assembly and activation and ATPase activity. The Journal of biological chemistry. 2009; 284:24891–903. [PubMed: 19589775]
32. Kusmierczyk AR, Kunjappu MJ, Funakoshi M, Hochstrasser M. A multimeric assembly factor controls the formation of alternative 20S proteasomes. Nature structural & molecular biology. 2008; 15:237–44.
33. Bohn S, et al. Structure of the 26S proteasome from Schizosaccharomyces pombe at subnanometer resolution. Proceedings of the National Academy of Sciences of the United States of America. 2010; 107:20992–7. [PubMed: 21098295]
34. Nickell S, et al. Insights into the molecular architecture of the 26S proteasome. Proceedings of the National Academy of Sciences of the United States of America. 2009; 106:11943–7. [PubMed: 19581588]
35. da Fonseca PC, Morris EP. Structure of the human 26S proteasome: subunit radial displacements open the gate into the proteolytic core. The Journal of biological chemistry. 2008; 283:23305–14. [PubMed: 18534977]
36. Andreasson C, Fiaux J, Rampelt H, Druffel-Augustin S, Bukau B. Insights into the structural dynamics of the Hsp110-Hsp70 interaction reveal the mechanism for nucleotide exchange activity. Proceedings of the National Academy of Sciences of the United States of America. 2008; 105:16519–24. [PubMed: 18948593]
37. Chen LL, Rosa JJ, Turner S, Pepinsky RB. Production of multimeric forms of CD4 through a sugar-based cross-linking strategy. The Journal of biological chemistry. 1991; 266:18237–43. [PubMed: 1917952]
38. Tomko RJ Jr, Funakoshi M, Schneider K, Wang J, Hochstrasser M. Heterohexameric ring arrangement of the eukaryotic proteasomal ATPases: implications for proteasome structure and assembly. Molecular cell. 2010; 38:393–403. [PubMed: 20471945]
39. Martin A, Baker TA, Sauer RT. Pore loops of the AAA+ ClpX machine grip substrates to drive translocation and unfolding. Nature structural & molecular biology. 2008; 15:1147–51.
40. Wang J, et al. Crystal structures of the HslVU peptidase-ATPase complex reveal an ATP-dependent proteolysis mechanism. Structure. 2001; 9:177–84. [PubMed: 11250202]
41. Bochtler M, et al. The structures of HsIU and the ATP-dependent protease HsIU-HsIV. Nature. 2000; 403:800–5. [PubMed: 10693812]
42. Kleijnen MF, et al. Stability of the proteasome can be regulated allosterically through engagement of its proteolytic active sites. Nature structural &molecular biology. 2007; 14:1180–8.
43. Chen C, et al. Subunit-subunit interactions in the human 26S proteasome. Proteomics. 2008; 8:508–20. [PubMed: 18186020]
44. Satoh K, Sasajima H, Nyoumura KI, Yokosawa H, Sawada H. Assembly of the 26S proteasome is regulated by phosphorylation of the p45/Rpt6 ATPase subunit. Biochemistry. 2001; 40:314–9. [PubMed: 11148024]
45. Hartmann-Petersen R, Tanaka K, Hendil KB. Quaternary structure of the ATPase complex of human 26S proteasomes determined by chemical cross-linking. Archives of biochemistry and biophysics. 2001; 386:89–94. [PubMed: 11361004]
46. Davy A, et al. A protein-protein interaction map of the Caenorhabditis elegans 26S proteasome. EMBO reports. 2001; 2:821–8. [PubMed: 11559592]
47. Zhang Z, et al. Structural and functional characterization of interaction between hepatitis B virus X protein and the proteasome complex. The Journal of biological chemistry. 2000; 275:15157–65. [PubMed: 10748218]

48. Gerlinger UM, Guckel R, Hoffmann M, Wolf DH, Hilt W. Yeast cycloheximide-resistant crl mutants are proteasome mutants defective in protein degradation. Molecular biology of the cell. 1997; 8:2487–99. [PubMed: 9398670]

49. Walz J, et al. 26S proteasome structure revealed by three-dimensional electron microscopy. Journal of structural biology. 1998; 121:19–29. [PubMed: 9573617]

50. Park S, Tian G, Roelofs J, Finley D. Assembly manual for the proteasome regulatory particle: the first draft. Biochemical Society transactions. 2010; 38:6–13. [PubMed: 20074027]

51. Leggett DS, et al. Multiple associated proteins regulate proteasome structure and function. Molecular cell. 2002; 10:495–507. [PubMed: 12408819]

52. Enemark EJ, Joshua-Tor L. Mechanism of DNA translocation in a replicative hexameric helicase. Nature. 2006; 442:270–5. [PubMed: 16855583]

53. Thomsen ND, Berger JM. Running in reverse: the structural basis for translocation polarity in hexameric helicases. Cell. 2009; 139:523–34. [PubMed: 19879839]

54. Davies JM, Brunger AT, Weis WI. Improved structures of full-length p97, an AAA ATPase: implications for mechanisms of nucleotide-dependent conformational change. Structure. 2008; 16:715–26. [PubMed: 18462676]

55. Rose, MD.; Winston, FM.; Heiter, P. Methods in yeast genetics: a laboratory course manual. Cold Spring Harbor Laboratory Press; Cold Spring Harbor, NY: 1990.

56. Finley D, Ozkaynak E, Varshavsky A. The yeast polyubiquitin gene is essential for resistance to high temperatures, starvation, and other stresses. Cell. 1987; 48:1035–46. [PubMed: 3030556]

57. Janke C, et al. A versatile toolbox for PCR-based tagging of yeast genes: new fluorescent proteins, more markers and promoter substitution cassettes. Yeast. 2004; 21:947–62. [PubMed: 15334558]

58. Schmidt M, et al. The HEAT repeat protein Blm10 regulates the yeast proteasome by capping the core particle. Nature structural & molecular biology. 2005; 12:294–303.

59. Leggett DS, Glickman MH, Finley D. Purification of proteasomes, proteasome subcomplexes, and proteasome-associated proteins from budding yeast. Methods in molecular biology. 2005; 301:57–70. [PubMed: 15917626]

60. Elsasser S, Schmidt M, Finley D. Characterization of the proteasome using native gel electrophoresis. Methods in enzymology. 2005; 398:353–63. [PubMed: 16275342]

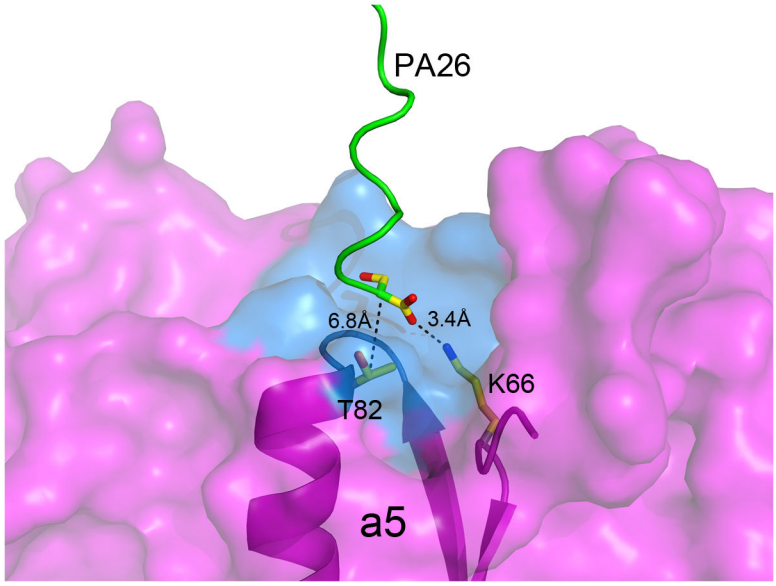

Figure 1.

Structural basis for the crosslinking strategy. Detail of a representative α pocket (α4–α5), showing residues used for crosslinking. A surface representation of the α5 subunit is shown along with cartoon representation of the last 12 residues of a PA26 subunit inserted in the α4–α5 pocket[9]. α5 is in purple, α4 in blue. A partial backbone of the α5 subunit is presented in cartoon mode with the side chain of T82 (the residue substituted with Cys and used for crosslinking) and K66 of α5 subunit as well as the C-terminal carbonyl group of PA26 presented in stick mode. The distance between the C-terminus of PA26 and the pocket lysine K66, as well as that between the C-terminus and T82, are labeled (PDB: 1FNT[11]).

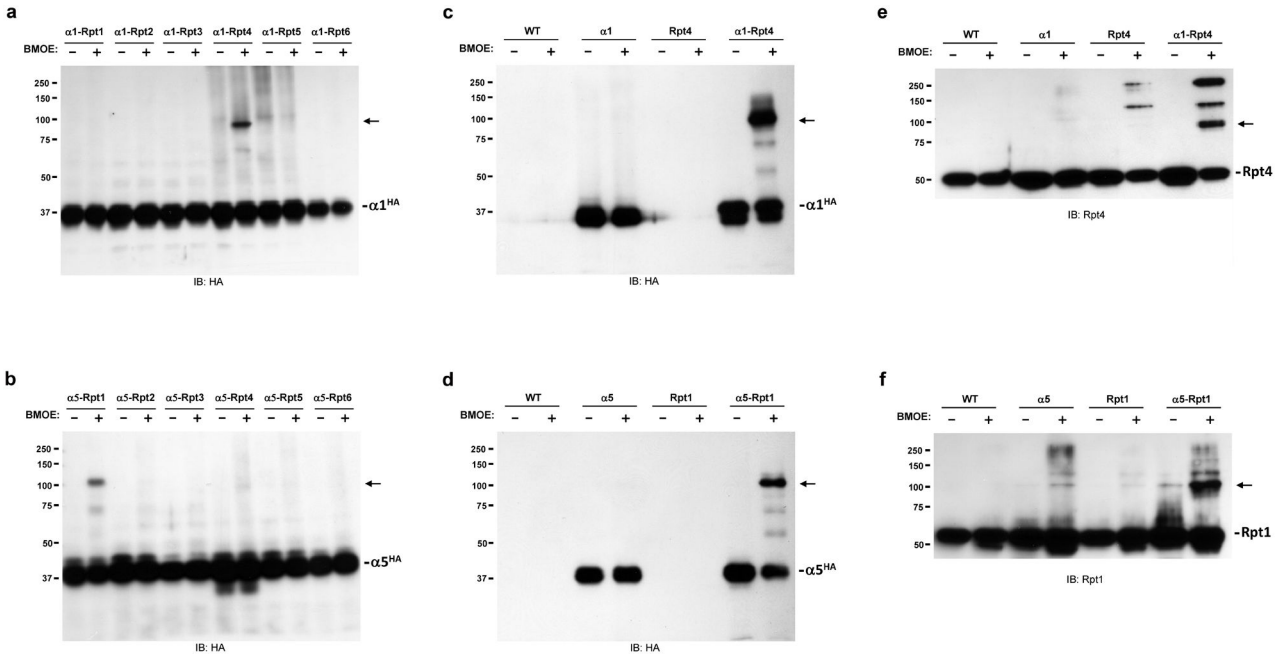

Figure 2.

Identification of two α–Rpt subunit pairs by cysteine crosslinking. **(a,b)** Whole cell lysates of yeast were subjected to crosslinking and SDS-PAGE-immunoblot analysis. In each panel, strains bear one α and one Rpt subunit with introduced cysteines. Panels **a** and **b** represent α1-I87C and α5-T82C mutants, respectively. Each panel contains a complete set of Rpt C-terminal mutants, as indicated (Rpt1-N467C, Rpt2-L437C, Rpt3-K428C, Rpt4-L437C, Rpt5-A434C, and Rpt6-K405C). A 6xHA tag is present at the C-terminus of each α subunit. BMOE (0.1 mM) is a cysteine-cysteine crosslinker; crosslinking proceeded for 1 hr at 4°C. Crosslinked products are marked by an arrow. The antibody used to probe each panel is indicated at bottom. The electrophoretic mobility and molecular mass (in kDa) of protein standards are indicated at left. **(c–f)** Purified proteasomes from wild type yeast or mutant yeasts with either a single cysteine substitution or a double cysteine substitution within the two α–Rpt pairs identified in panels **a** and **b** were subjected to crosslinking and SDS-PAGE-immunoblot analysis. Panels **c** and **e** for α1–Rpt4; panel **d** and **f** for α5–Rpt1. Here, as below, proteasomes were purified via a Protein A tag appended to Rpn11(ref. 51).

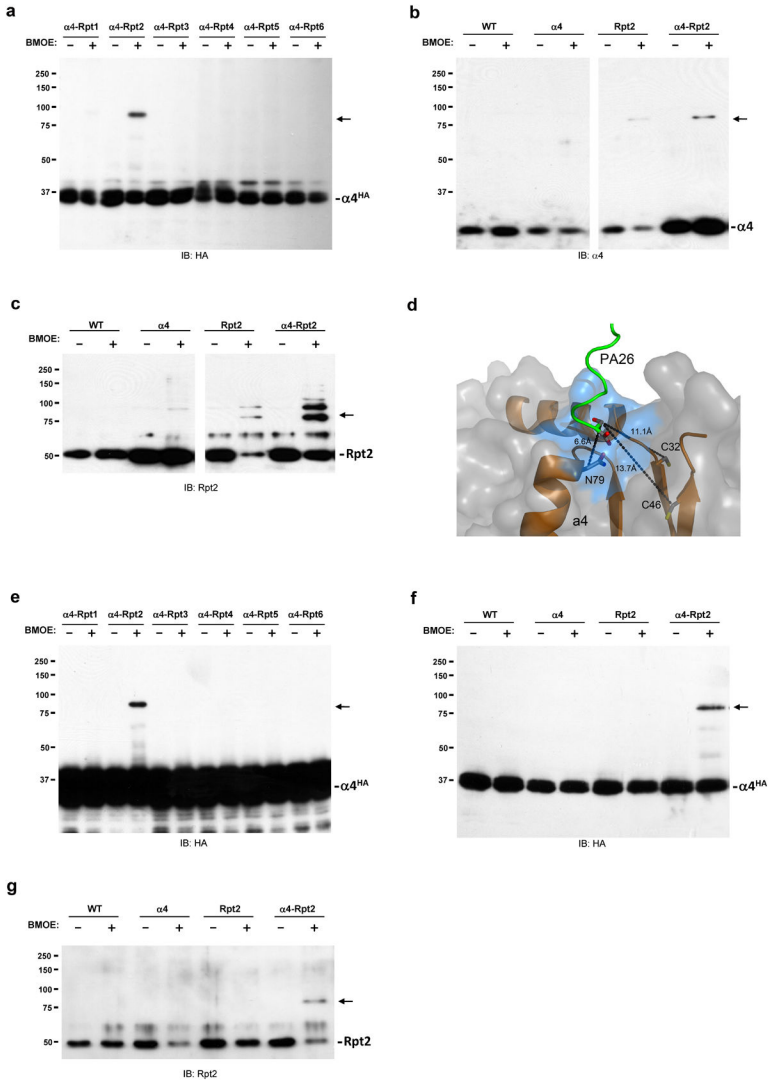

Figure 3.

Identification of the α4–Rpt2 pair. **(a)** Whole cell lysates from α4-N79C RptX double mutants were subjected to crosslinking and SDS-PAGE-immunoblot analysis. See legend to panel **2a** for details. The crosslinked product is marked by an arrow. The antibody used to probe each panel is indicated at bottom. **(b,c)** Crosslinking of α4 to Rpt2 does not strictly require an introduced cysteine in α4. Purified proteasomes from wild type or mutant yeast with either single or double cysteine substitutions of the Rpt2–α4 pair were crosslinked and subjected to SDS-PAGE-immunoblot analysis. A set of strains in which the α4 subunit was not HA-tagged was used here and the blot was probed with α4-specific antibody. **(d)** Model of the α3–α4 pocket, showing proximity of endogenous Cys residues (C32 and C46) to the pocket. The surface of α4 is in gray. Cartoon representation of partial backbone of α4 and the C-terminal tail of PA26 are presented in red and green respectively, whereas the pocket surface is highlighted in blue. C32 and C46, along with N79 and C-terminus of PA26, are represented in stick mode and the distances between their β-carbons are labeled (PDB: 1FNT[11]). **(e)** Whole cell lysates from cells expressing HA-tagged wild type α4 and Cys-

substituted Rpt proteins were subjected to crosslinking, followed by SDS-PAGE-immunoblot analysis. See legend to panel **3a** for details. **(f,g)** Purified proteasomes from a set of C32A C46A strains were subjected to crosslinking followed by SDS-PAGE-immunoblot analysis. In lanes marked α4, N79 was substituted with Cys. Those marked Rpt2 are from Rpt2-L437C mutants.

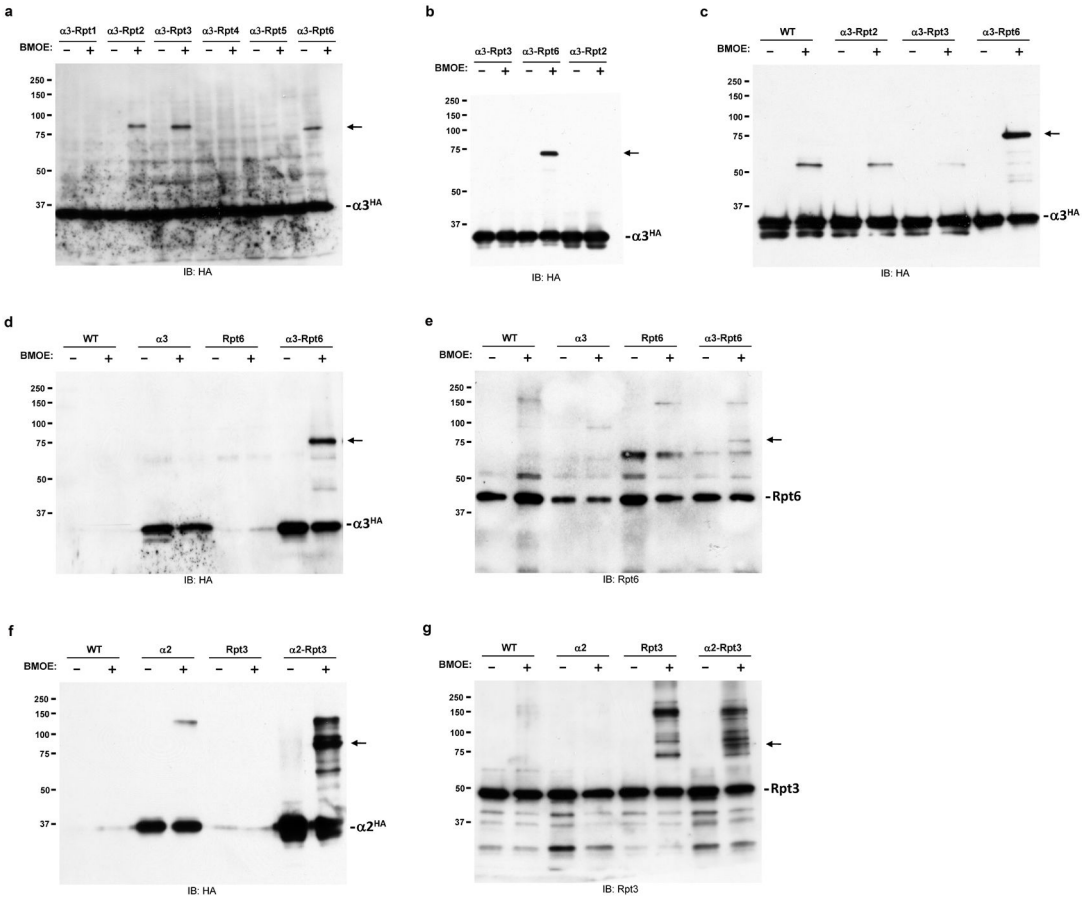

Figure 4.

Identification of the α3–Rpt6 and α2–Rpt3 pairs. **(a)** Whole cell lysates from stationary-phase yeast strains carrying double Cys substitutions as indicated were subjected to crosslinking and SDS-PAGE-immunoblot analysis. All strains expressed α3-T81C. For the Rpt mutant set, see legend to Fig. 2a. Antibody to HA was used to probe for crosslinked products. **(b)** Whole cell lysates from yeast strains carrying the three identified Rpt–α3 pairs of panel **a** and in exponential growth ($O.D._{600}$=1) were subjected to crosslinking and SDS-PAGE-immunoblot analysis. **(c)** Purified proteasomes from wild type yeast or mutant yeasts with either a single cysteine substitution or a double cysteine substitution within the α3–Rpt6 pair identified in panels **a** and **b** were subjected to crosslinking and SDS-PAGE-immunoblot analysis. **(d,e)** Purified proteasomes were subjected to crosslinking and SDS-PAGE-immunoblot analysis. Mutant samples were α3-T81C, Rpt6-K405C, and α3-T81C Rpt6-K405C. The blots were probed with antibodies to either HA (to detect α3) or Rpt6. **(f,g)** Purified proteasomes were subjected to crosslinking and SDS-PAGE-immunoblot analysis. Mutant proteins were α2-A79C, Rpt3-K428C, and α2-A79C Rpt3-K428C. Blots were probed with antibodies to either HA or Rpt3. **(g)** Similar to Fig. 2a but with purified proteasomes from a set of strains bearing α2-A79C with Rpt C-terminal mutants. The blot was probed for possible crosslinked product using antibodies to Rpt3.

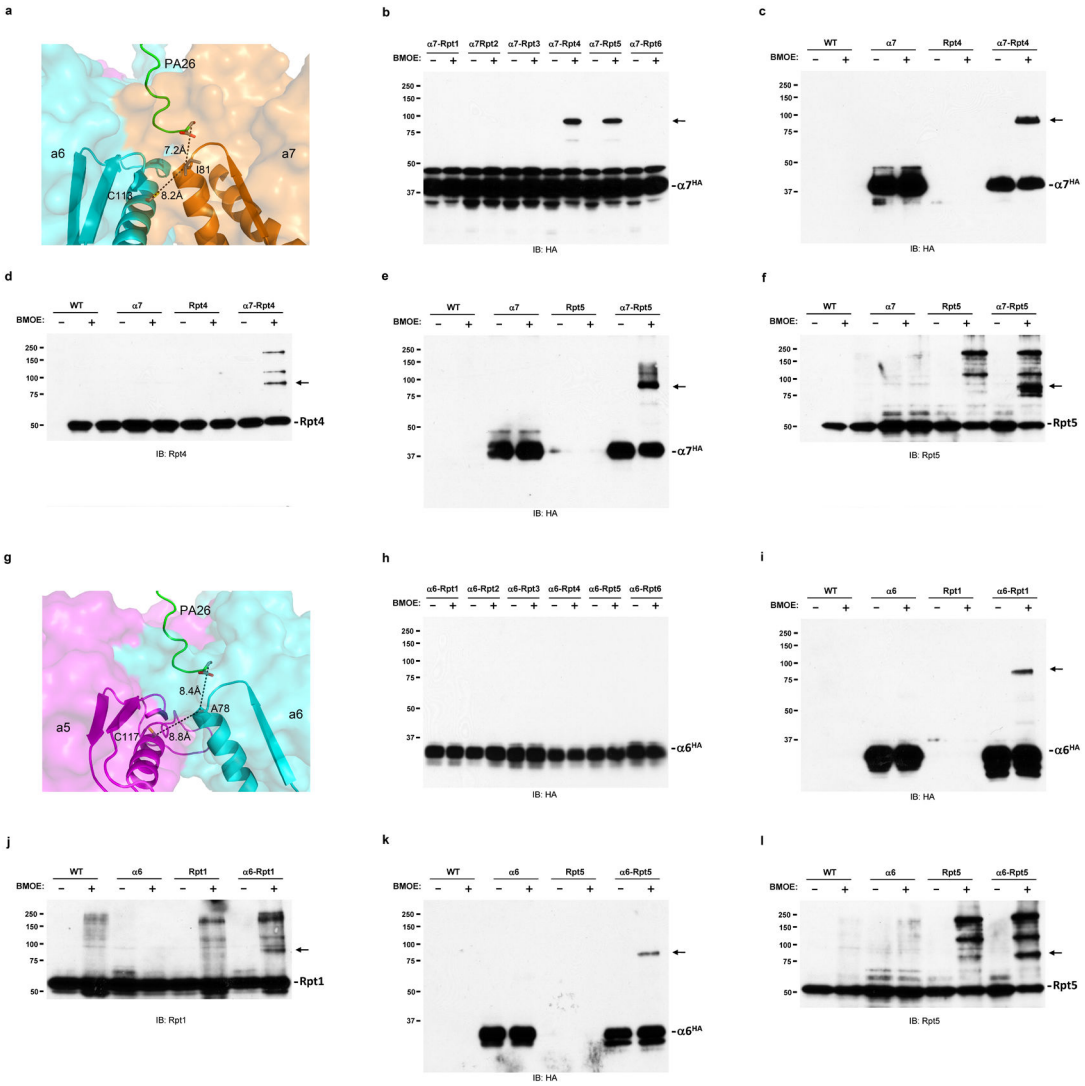

Figure 5.

Identification of crosslinks for α5–α6 and α6–α7 pockets. **(a)** Model of the α6–α7 pocket showing proximity of endogenous residue C113 of α6 to the introduced cysteine (A78C). The two α subunits were painted in magenta and cyan respectively and the C-terminus of PA26 in green. Partial backbones of the α subunits are in cartoon mode. Side chains of the three residues, either with native cysteine or the introduced cysteine, are in stick mode and the distances between their β-carbons are labeled. **(b)** Whole cell lysates from yeast strains carrying double Cys substitutions as indicated were subjected to crosslinking and SDS-PAGE-immunoblot analysis. All strains expressed α7-I81C with C113 of α6 mutated to alanine. For the Rpt mutants, see legend to Fig.2a. (c,d) Purified proteasomes were subjected to crosslinking and SDS-PAGE-immunoblot analysis. Mutant samples were α7-I81C, Rpt1-N467C, and α7-I81C Rpt1-N467C, all of which are purified from strains with C113 of α6 substituted with alanine. **(e,f)** As in **c** and **d**, except for confirmation of α7-I81C and Rpt5-A434C crosslinking. **(g)** Similar to **a**, model of α5–α6 pocket to show proximity of native cysteine C117 in α5 to the position where a cysteine was introduced in α6. α5 was painted

in magenta while the others are in the color scheme of **a. (h)** As in b, crosslinking of whole cell lysates of a set of strain bearing the α6-A78C and α5-C117A mutations. For Rpt mutants, see legend to Fig. 2a. (i–l) Similar as **c–f**, except that crosslinking was carried out with α6-A78C and Rpt4-L437A or Rpt5-A434C mutants.

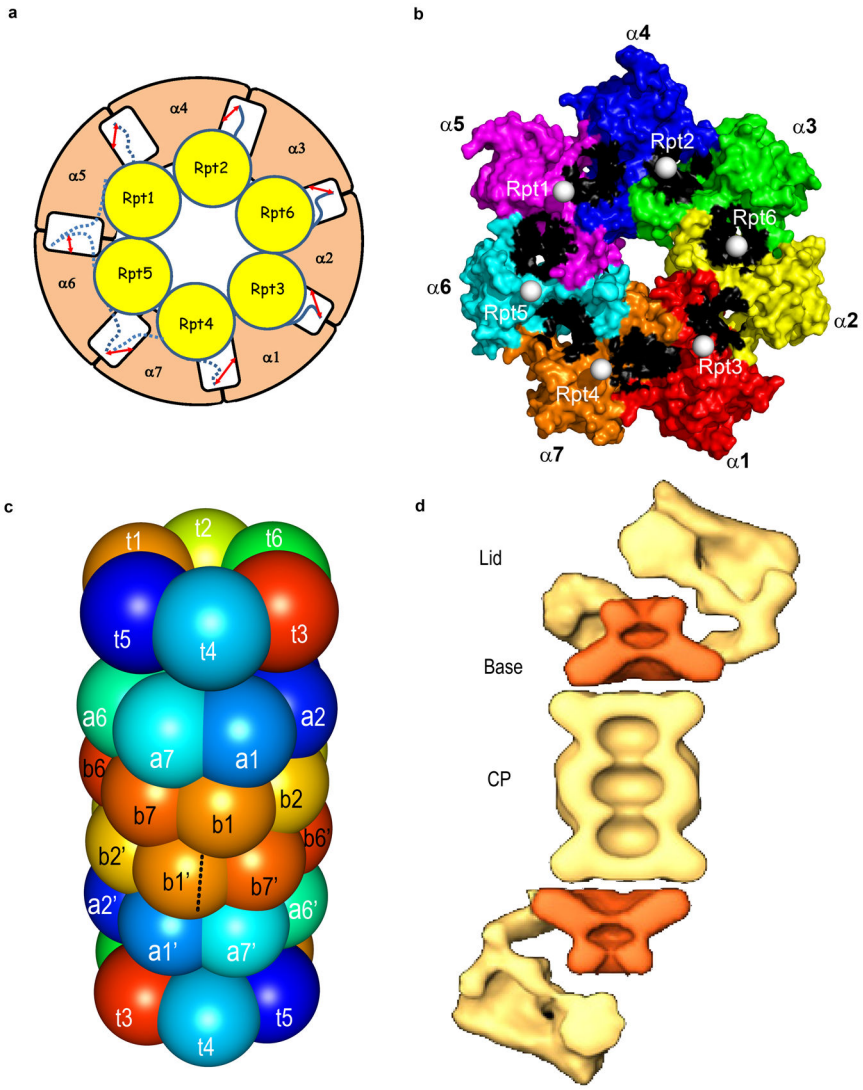

Figure 6.

Model of the base–CP complex. **(a)** Proposed model mapping the six Rpt tails to the seven α-pockets of the CP. α subunits are in tan with white inter-subunit pockets. Rpt subunits are in yellow with blue C-terminal tails. Solid arrows from an Rpt's C-terminal tail represent unique crosslinking between Rpt and specific α pocket. Dashed arrows from the C-terminal tail indicate crosslinking of Rpt to multiple α pockets. **(b)** Proposed model for the mapping the six Rpt tails into the seven α-pockets of the CP. The α-ring is represented as a molecular surface mode with each subunit in a different color. The pockets formed between subunits are colored black. The six Rpt C-termini are given as white spheres, the positions of which are modeled from the C-termini of the D2 domain of CDC48 (PDB: 3CF1 ref. 54). **(c)** Ball model of base–CP complex. The C2-fold symmetry axis of the CP lies at the interface between β1 and β1′ as shown. **(d)** CP-RP misalignment of the proteasome holoenzyme as revealed by cryo-electron microscopy. Averaged images of negatively stained *Drosophila melanogaster* proteasomes. The density assigned to the Rpt ring is given in orange, the remainder of the proteasome in tan. Adapted with permission from Nickell et al[34].

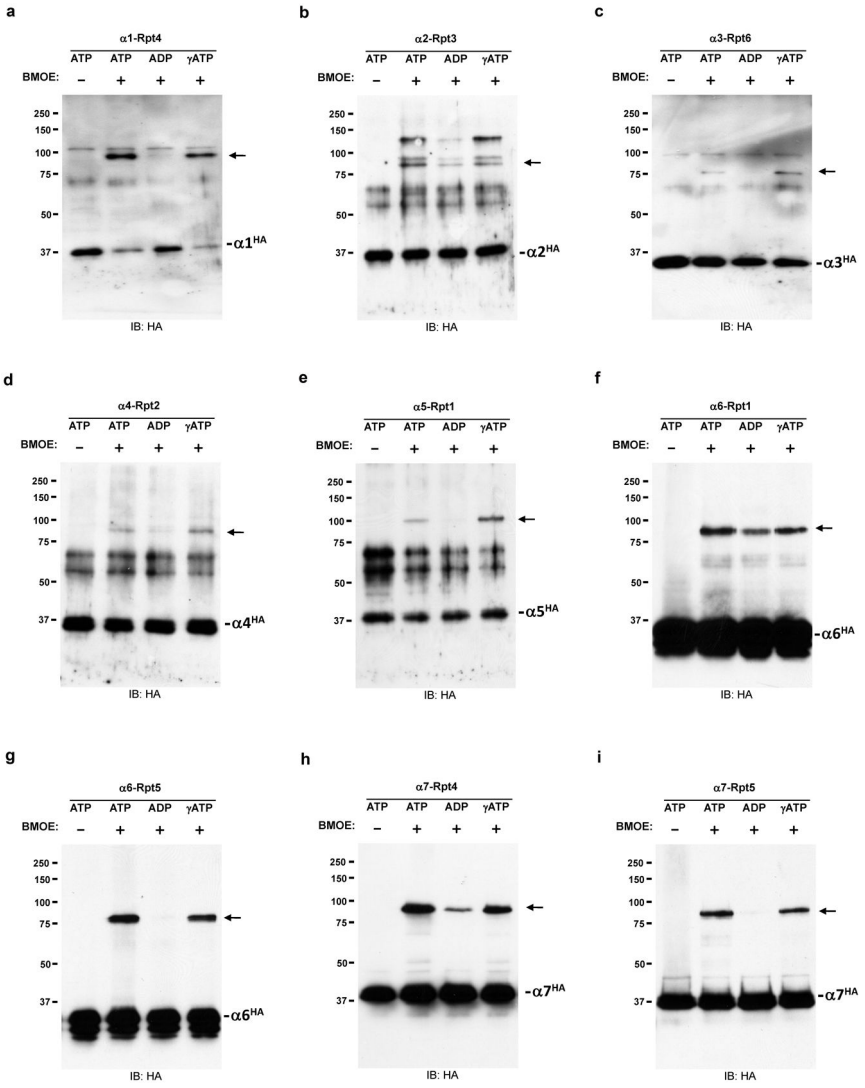

Figure 7.

Effect of nucleotides on crosslinking between α and Rpt subunits. Proteasomes with introduced cysteines on the nine identified α–Rpt pairs were purified in the presence of 0.1 mM ATP, then incubated at room temperature for 30 min with various nucleotides as indicated at 1 mM, followed by crosslinking at 4°C. Immunoblots of these samples were probed with antibody to HA.

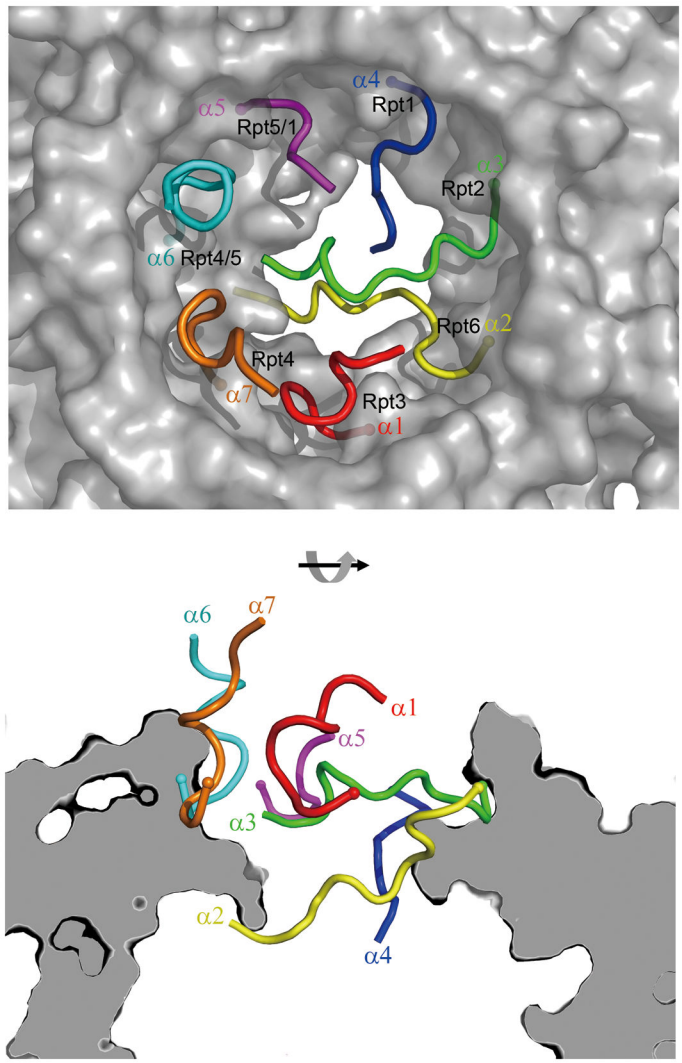

Figure 8.

α-subunit N-terminal tails and the Rpt proteins proposed to direct their movements. Top panel as viewed from the RP–CP interface. The closed form of the CP channel is shown[4]. The N-terminal tails (residues 10–18 of α1, 1–11 of α2, 2–12 of α3, 3–10 of α4, 9–14 of α5, 2–12 of α6, and 4–13 of α7) are shown in cartoon mode and painted in different colors. The remaining residues are in surface representation, colored in grey. The α carbon of the last residue of each N-terminal tail is in sphere mode. The bottom panel is a side view of the α-ring gate with the same color scheme as at top. Note that Rpt4 and Rpt6 are positioned to disrupt the N-terminal tails of α7 and α2, but do not open the gate[29], consistent with their lack of a HbYX motif[8] and the minor role in gating played by the peripheral α7 N-terminus[12].